Crystallization Behaviors of Linear and Long Chain Branched Polypropylene

Jinghua Tian, Wei Yu, Chixing Zhou

Department of Polymer Science and Engineering, Advanced Rheology Institute, Shanghai Jiao Tong University, Shanghai 200240, People's Republic of China

Received 13 September 2006; accepted 29 November 2006
DOI 10.1002/app.26024
Published online in Wiley InterScience (www.interscience.wiley.com).

ABSTRACT: The nonisothermal crystallization kinetics of linear and long chain branched polypropylene (LCB PP) were investigated by differential scanning calorimetry (DSC) at various cooling rates. Several methods such as Avrami, Ozawa, and Jeziorny were applied to describe the crystallization process of linear PP and LCB PPs with different LCB level under nonisothermal conditions. The values of $t_{1/2}$, Z_c, and $F(T)$ show that LCB has the role of heterogeneous nucleating agent and accelerates the crystallization process of PP. Moreover, the Kissinger method was used to evaluate the activation energy of linear PP and LCB PPs. The result shows that the activation energy of LCB PPs are higher than that of linear PP, indicating that the presence of LCB baffles the transfer of macromolecular segments from PP melt to the crystal growth surface. Furthermore, the crystal morphology of linear PP and LCB PPs was observed through polarized optical microscopy (POM), and fine spherulites were observed for LCB PPs. © 2007 Wiley Periodicals, Inc. J Appl Polym Sci 104: 3592–3600, 2007

Key words: polypropylene; long chain branch; nonisothermal crystallization; kinetic

INTRODUCTION

Isotactic polypropylene (iPP) has many desirable and beneficial physical properties such as low density, high melting point, and chemical resistance. Therefore, iPP has been used widely in industrial and commercial applications. However, iPP is a linear polymer, as a result, it exhibits low melt strength and no strain hardening behavior in the melt state, which limits its use in applications such as thermoforming, foaming, and blow molding. The most effective method to improve the melt strength of PP is to introduce long chain branching (LCB) onto the PP backbone.[1–5] There has been considerable interest in the relationships between LCB molecular architecture and rheological behavior of PP in the recent years.[4–7] The change of molecular architecture can affect not only rheological property but also crystallization property of PP. However, the crystallization behavior of linear and long chain branched polypropylene (LCB PP) has seldom been studied in detail.

There have many studies on the crystallization of grafted PP. It is widely accepted that grafted PP partly acts as a nucleating agent for the matrix and accelerates the crystallization rate. Güldoğan et al.[8] and Seo et al.[9] speculated that the different crystallization behavior between PP-*g*-MA and PP is due to a chain interaction, such as hydrogen bonding between hydrolyzed maleic anhydride groups. There is no specific definition about LCB, however, from rheological viewpoint, the length necessary for a branch to behave as a long chain branch is $2M_e$ (M_e = molecular weight between entanglements).[3,6,10,11] Therefore, the molecular architectures for grated PP and LCB PP are very different. As a result, the crystallization behavior and crystal morphology of LCB PP will be different from linear PP or grafted PP. It can be concluded from limited literatures[2,12] that LCB PP has higher crystallization temperature, shorter crystallization time, and broader melting range when compared with linear PP.

In our previous study,[13] LCB PPs with different LCB level were prepared by melt grafting in the presence of peroxide and polyfunctional monomer, and their linear viscoelastic properties were also studied. The purpose of this article is to investigate the nonisothermal crystallization kinetics of LCB PPs with different LCB level compared with linear PP. Several nonisothermal crystallization kinetic equations were used. The necessary data were obtained from differential scanning calorimetry (DSC) thermogram. The kinetic parameters such as the Ozawa exponent and the activation energies were calculated. In addition, the crystal morphology of linear PP and LCB PPs was also studied by polarized optical microscopy (POM).

Correspondence to: W. Yu (wyu@sjtu.edu.cn).
Contract grant sponsor: Natural Science Foundation of China; contract grant numbers: 50390095, 20574045.

TABLE I
Formulation, Zero-Shear Viscosity and LCB Level of Samples

Samples	Irganox 1010 (phr)	Peroxide (phr)	PETA (phr)	$\eta_0 \times 10^4$ Pa s	LCB/10^4 C
PP	0.2	–	–	2.00	–
D1	0.2	0.1	0.6	1.85	0.025
D2	0.2	0.1	2.0	3.62	0.38
D3	0.2	0.1	4.0	4.57	>0.38

EXPERIMENTAL

Sample preparation

LCB PPs with different LCB level were prepared by melting grafting in the presence of 2,5-dimethyl-2,5(*t*-butylperoxy) hexane peroxide and pentaerythritol triacrylate (PETA) polyfunctional monomer in mixer at 180°C; the details of the preparation process and characterization by rheology methods were discussed in Ref. 15. The formulation, zero-shear viscosity, and LCB level of samples were listed in Table I, where η_0 and LCB/10^4C were determined by rheology method. LCB level of D3 cannot be calculated accurately because its longer relaxation time is larger than the maximum relaxation time that can be determined from our experiments. However, it can be confirmed that LCB level of D3 is higher than that of D2.

Differential scanning calorimetry

Thermal analysis of the samples was carried out with a differential scanning calorimeter (DSC) instrument (model Pyris 1, PerkinElmer, USA) under nitrogen atmosphere. To study the crystallization and melting behaviors, the samples about 4 mg were melted at 200°C for 5 min to eliminate thermal history, followed by cooling at a rate of 10°C/min and the crystallization thermogram was measured. The temperature of peaks was taken as the crystallization temperature, T_c. As soon as the temperature reached 50°C, it was reheated again at a rate of 10°C/min and the melting thermogram was measured. The temperature of peak and area of the endothermic curve were taken as the melting temperature, T_m, and the heat of fusion, ΔH_f, respectively.

The procedure for nonisothermal crystallization was as follows: the samples were melted at 200°C for 5 min to eliminate thermal history, and then cooled to room temperature at 5, 10, 20, 30, and 40°C/min, respectively. The exothermal curves of heat flow as a function of temperature were recorded to analyze the nonisothermal crystallization process of PP and LCB PPs.

Polarized optical microscopy

The crystal morphology of the linear PP and LCB PPs was studied on thin films about 0.1 mm by a Leica DMLP (Linkam Scientific Instruments, Britain) optical polarizing microscope with an automatic hot-stage thermal control. A sample was sandwiched between two microscope cover glasses, melted at 200°C for 5 min to eliminate thermal history, and then cooled to room temperature at 20°C/min.

RESULTS AND DISCUSSION

Crystallization and melting behavior of PP and LCB PPs

Figure 1(a,b) shows cooling and heating thermograms of PP and LCB PPs, and the corresponding crystallization and melting parameters determined from Figure 1

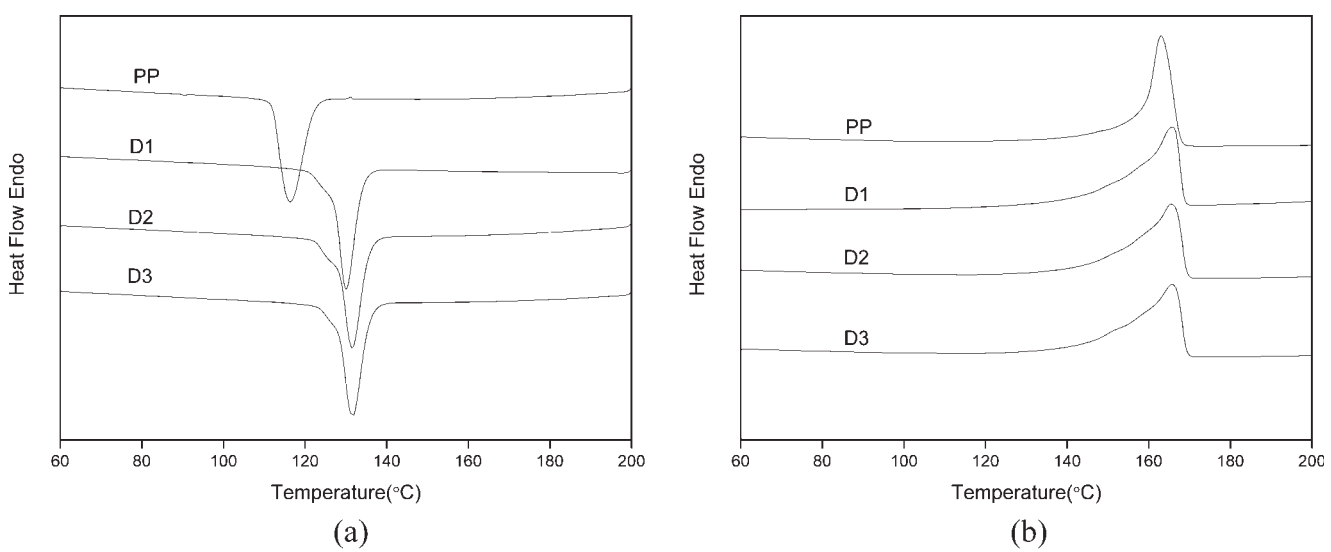

Figure 1 DSC cooling thermograms (a) and melting thermograms (b) for PP and LCB PPs at 10°C/min.

TABLE II
Melting and Crystallization Parameters of PP and LCB PPs

Samples	PP	D1	D2	D3
T_m (°C)	163.1	165.8	165.4	165.7
T_c (°C)	115.3	130.8	132.0	132.1
ΔH_c (J/g)	87.8	94.2	95.9	97.5
X_c (%)	42.0	45.1	45.9	46.6

are given in Table II. It can be seen from cooling thermograms in Figure 1(a) that the crystallization temperatures (T_c) of LCB PPs are higher than that of PP. As shown in Table II, T_c of PP is 115.3°C and T_c of D1, D2, and D3 is 130.8, 132.0, and 132.1°C, respectively. It is clear that the presence of LCB structure makes T_c of PP improve more than 15°C, however, T_c increases slightly with LCB level. Furthermore, in case of LCB PPs, a small shoulder on the cooling thermograms can be observed. It can be believed that the shoulder related to the presence of LCB structure, which will be discussed later.

The subsequent reheating thermograms of PP and LCB PPs are shown in Figure 1(b). The melting temperature (T_m) and the enthalpies of fusion (ΔH_m) are also listed in Table II. It can be seen that the thermograms for PP and LCB PPs all showed single melting peak. T_m of LCB PPs shift to higher temperature compared with that of PP, moreover, the shape of melting peaks for LCB PPs is broader than that of PP, which suggests that the crystallines of PP are more perfect than that of LCB PPs.

The crystallinity of PP can be determined from heating scans using the following equations:

$$X_c = \frac{\Delta H_f}{\Delta H_f^0} \times 100\% \quad (1)$$

where ΔH_f is the specific enthalpy of melting of the samples and ΔH_f^0 is the melt enthalpy of the hypothetically 100% crystalline polypropylene ($\Delta H_f^0 = 209$ J/g).[14] The crystallinity of PP and LCB PPs was calculated by eq. (1) and the data were listed in Table II. As shown in Table II, the crystallinity of LCB PPs is higher than that of PP, indicating that the branched chains can act as a nucleating agent and help to increase the crystallinity of PP.

Nonisothermal crystallization behavior of PP and LCB PPs

Figure 1 shows the nonisothermal crystallization exothermal curves of PP and LCB PP (sample D2) at different cooling rates. Some useful parameters such as the onset crystallization temperature (T_o), the peak temperature (T_p), and the end crystallization temperature (T_e) can be obtained from these curves, and the values were listed in Table III. As expected, the exothermic peak shifted to lower temperature and became broader with cooling rate increasing for all samples. As shown in Table III, T_p of LCB PPs is higher than that of PP at given cooling rate, indicating that the crystallization rate increased and the degree of supercooling required for the crystallization reduced when LCB was introduced onto PP backbone. Moreover, at the given cooling rate, T_p increased slightly with LCB level increasing; however, it almost does not change again when LCB level achieved a given value, i.e., D2. In addition, a small shoulder appeared on the LCB PPs cooling curves at lower temperature and became unconspicuous with the increasing cooling rate. To our knowledge, this phenomenon was not reported in other linear, grafted, or branched polymers. The exact reason was not known, but it can be certain that the shoulder is related to the presence of LCB structure, which influences the crystallization kinetic process of PP. This phenomenon will be discussed in following analysis of nonisothermal crystallization kinetic parameters.

Nonisothermal crystallization kinetics of linear PP and LCB PPs

Although most of the research work was devoted to the crystallization of polymers under isothermal conditions, it is important to investigate nonisothermal crystallization kinetics of crystalline polymers because actual processing of polymers is more likely to proceed under nonisothermal conditions.

TABLE III
Parameters Determined from the DSC Exothermal Curves

Samples	ϕ (°C/min)	T_o (°C)	T_p (°C)	T_e (°C)
PP	5	124.2	119.6	116.4
	10	120.9	115.3	111.9
	20	117.1	110.9	106.9
	30	115.2	108.9	104.1
	40	113.3	106.3	100.9
D1	5	138.1	134.4	131.6
	10	134.8	130.8	127.6
	20	131.3	127.3	122.9
	30	129.0	124.4	118.3
	40	127.6	122.9	117.8
D2	5	139.6	135.7	132.8
	10	136.0	132.0	128.7
	20	132.4	128.2	124.2
	30	130.5	125.9	121.0
	40	128.6	123.5	116.9
D3	5	139.7	135.5	131.7
	10	136.3	132.1	127.8
	20	132.7	128.2	122.9
	30	130.4	125.4	117.9
	40	128.8	123.5	114.0

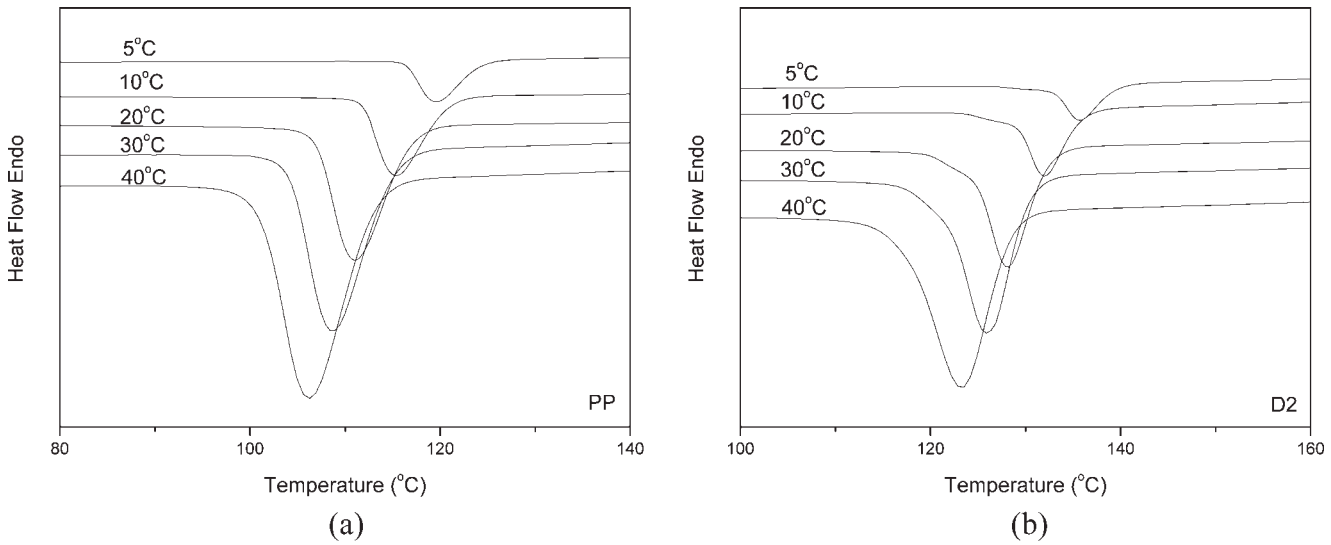

Figure 2 DSC patterns for PP and LCB PPs during the nonisothermal crystallization at different cooling rates: (a) PP; (b) D2.

Integration of the exothermal peaks during the nonisothermal scan can also give the relative crystallinity as a function of temperature or time as isothermal crystallization. In the nonisothermal crystallization, the time t has the relation with the temperature T as follows:

$$t = \frac{T_o - T}{\phi} \tag{2}$$

where T is the temperature at time t, T_o is the onset crystallization temperature, and ϕ is the cooling rate.

The development of relative crystallinity as a function of temperature during nonisothermal crystallization for PP and LCB PP at different cooling rates was shown in Figure 3. All these curves have the similar reversed S shape, indicating that only the retardation effect of cooling rate on the crystallization was observed in these curves.[15] However, a slower transition responding to the shoulder in Figure 1(b) occurred at the later crystallization stage for LCB PPs. According to eq. (2), the relationship between relative crystallinity and time can be obtained as shown in Figure 4. The results show that the crystallization time became shorter with cooling rate increasing for all samples. The half-time of nonisothermal crystallization obtained from Figure 4 were listed in Table IV. As expected, the value of $t_{1/2}$ decreases with cooling rate increasing for PP and LCB PPs. Furthermore, at a given cooling rate, the

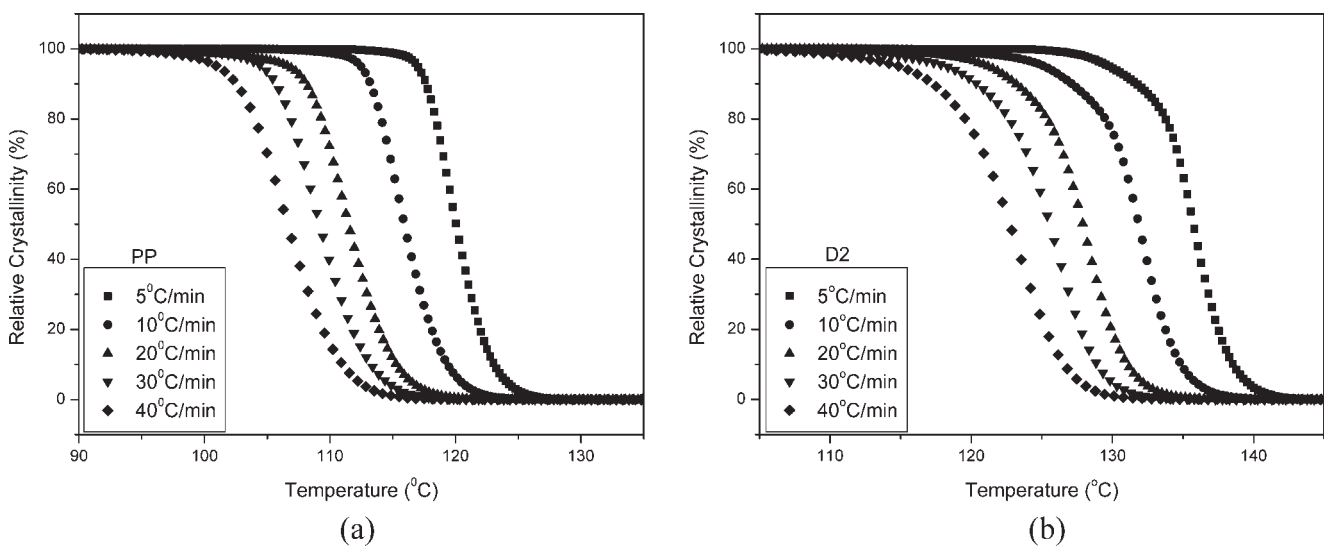

Figure 3 The curves of relative crystallinity versus temperature for PP and LCB PP: (a) PP; (b) D2.

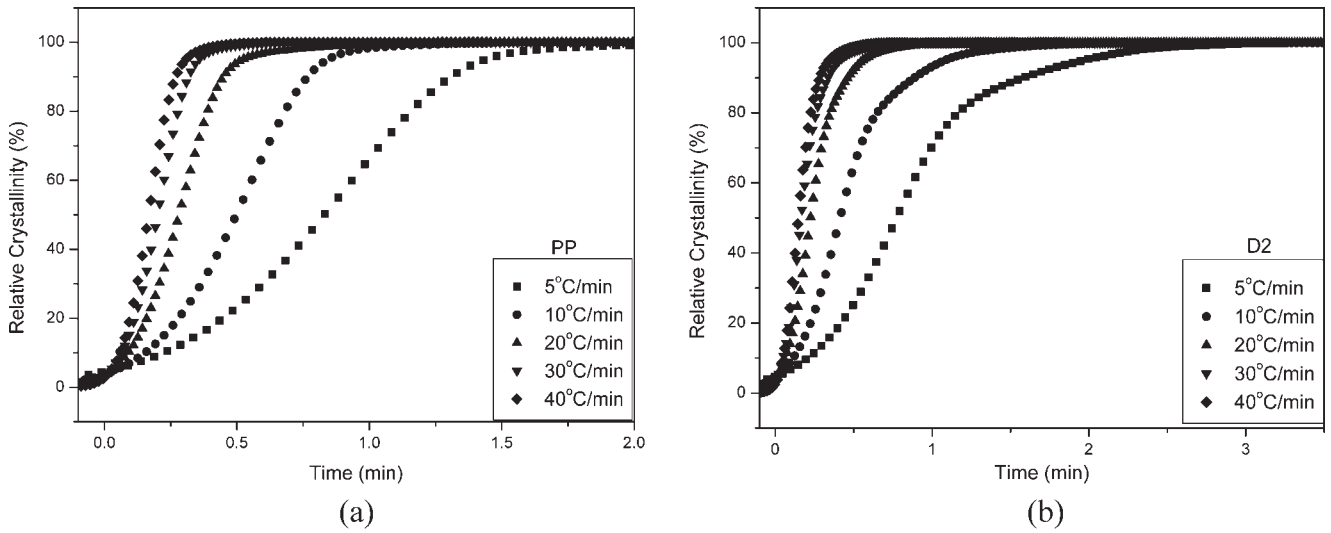

Figure 4 The curves of relative crystallinity versus time for PP and LCB PP: (a) PP; (b) D2.

value of $t_{1/2}$ for LCB PPs was lower than that for PP, indicating that the presence of LCB accelerated the crystallization process of PP.

On the basis of the assumption that the crystallization temperature is constant, the Avrami equation can be directly used to describe the primary stage of nonisothermal crystallization.[16] In this case, the Avrami equation is expressed as

$$1 - X(t) = \exp(-Z_t t^n) \tag{3}$$

where Z_t is the rate constant in the nonisothermal crystallization process, n is a mechanism constant depending on the type of nucleation, and growth process parameters. The double-logarithmic form of eq. (3) is

$$\log[-\ln(1 - X(t))] = \log Z_t + n \log t \tag{4}$$

Considering the nonisothermal character of the process investigated, the final form of the parameter characterizing the kinetics of nonisothermal crystallization was given by Jeziorny.[17]

$$\ln Z_c = \ln Z_t / \phi \tag{5}$$

where Z_t is the crystallization rate constant and Z_c is the modified crystallization rate constant considering cooling rate ϕ. Plots of $\log[-\ln(1 - X(t))]$ vs. $\log t$ were shown in Figure 5. Each curve shows only the linear portion, and the nonlinear part that deviated from Avrami equation at high relative crystallinity region was not included. Z_t and n were obtained from the intercept and slope, respectively, while Z_c was estimated according to eq. (5). The values of n and Z_c were listed in Table IV. The value of n varied from 2.36 to 2.82 for PP, while it varied from 1.94 to 2.07, 1.98 to 2.09, and 1.95 to 2.03 for D1, D2, and D3, respectively. In polymer crystallization from an entangled melt, noninteger values of n are often obtained, indicative of an overlap of different crystal growth geometries.[11] The exponent n of LCB PPs was smaller than that of PP at every cooling rate, indicating that the introduction of LCB influenced the mechanism of nucleation and the crystal growth geometry of PP. The larger the rate parameter Z_c value, the higher the crystallization rate is. At given cooling rate, Z_c of LCB PPs was higher than that of PP and $t_{1/2}$ of LCB PPs was lower than that of PP, suggesting that branches can play as heterogeneous nucleating agent and accelerate the crystallization

TABLE IV
Nonisothermal Crystallization Kinetic Parameters from the Avrami and Jezioney Analysis

Samples	ϕ (°C/min)	n	Z_c	$t_{1/2}$ (min)
PP	5	2.63	0.1191	0.83
	10	2.82	0.3690	0.50
	20	2.54	0.6871	0.28
	30	2.53	0.8011	0.20
	40	2.36	0.8655	0.16
D1	5	1.94	0.2128	0.74
	10	2.07	0.4989	0.40
	20	1.99	0.7594	0.22
	30	1.96	0.8472	0.18
	40	2.02	0.8954	0.12
D2	5	2.05	0.1923	0.77
	10	2.05	0.4989	0.54
	20	2.09	0.7482	0.22
	30	1.98	0.8485	0.16
	40	2.04	0.8866	0.15
D3	5	2.00	0.1888	0.89
	10	2.01	0.4954	0.46
	20	2.03	0.7447	0.25
	30	1.96	0.8414	0.19
	40	1.95	0.8872	0.16

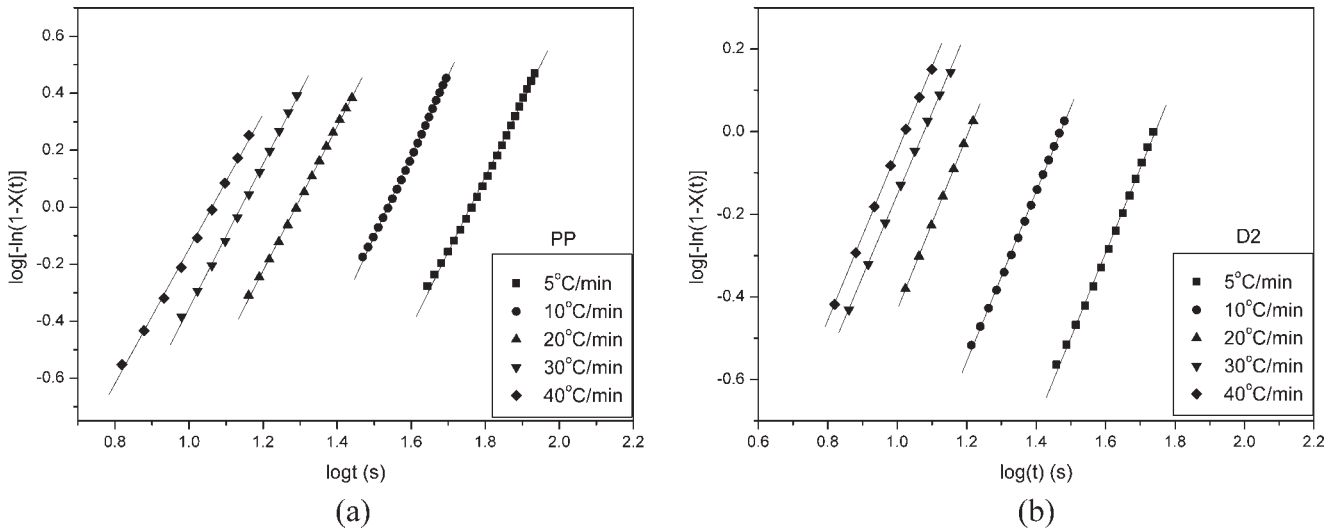

Figure 5 Plots of log[−ln(1 − X(t))] vs. log t for PP and LCB PP: (a) PP; (b) D2.

process of PP. In addition, the value of n for PP decreased gradually with cooling rate increasing, whereas the value of n for LCB PPs was influenced weakly by cooling rate, which means the dependence of the crystallization kinetics on the cooling rate is much weaker for LCB PP than for PP. n depends on the type of nucleation and the form of crystalline growth, so this result can be ascribed to the heterogeneous nucleation of LCB PP, which is less cooling rate dependent compared to homogeneous nucleation because heterogeneous nucleation forms simultaneously as soon as the sample reaches the crystallization temperature.

To study kinetic parameters for nonisothermal crystallization processes, several methods have been developed and the majority of the proposed formulations are based on the Avrami equation. Assuming that the nonisothermal crystallization process may be composed of infinitesimally small isothermal crystallization steps, Ozawa[18] extended the Avrami equation to the nonisothermal case as follows:

$$X(T) = 1 - \exp(-K(T)/\phi^m) \tag{6}$$

where $K(T)$ is the function of cooling rate, ϕ is the cooling rate, and m is the Ozawa exponent, which depends on the dimension of the crystal growth. The double-logarithmic form of eq. (6) is

$$\ln[-\ln(1 - X(T))] = \ln K(T) - m \ln \phi \tag{7}$$

Plots of ln[−ln(1 − X (T))] vs. ln ϕ for PP and LCB PP were shown in Figure 6(a,b), respectively. Good

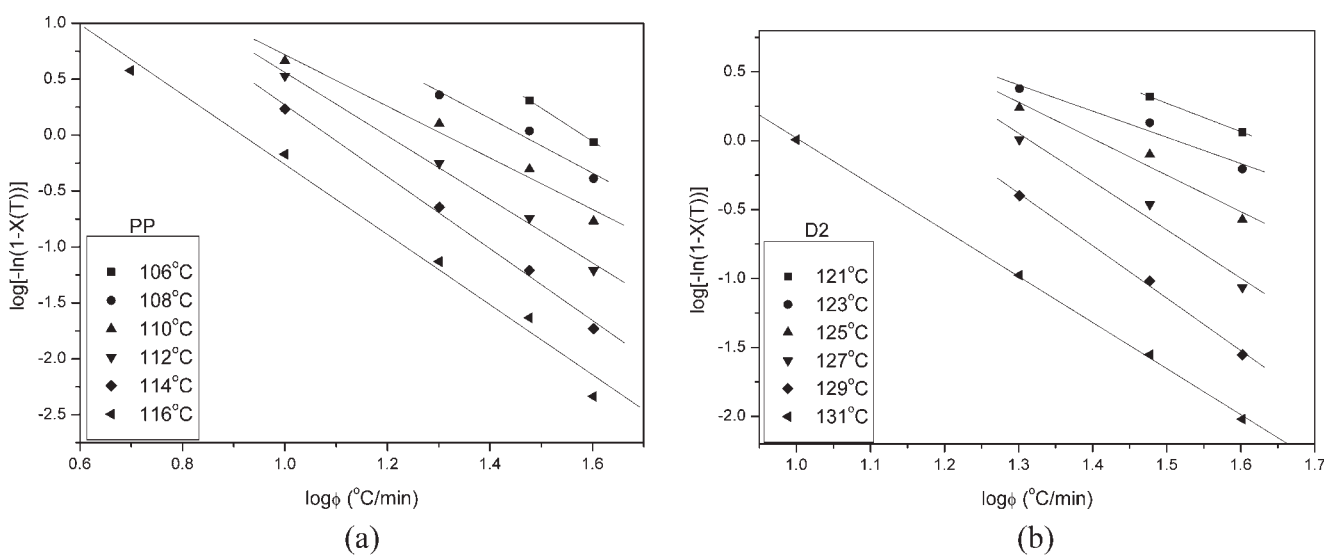

Figure 6 Plots of log[−ln(1 − X(t))] vs. log ϕ for PP and LCB PP: (a) PP; (b) D2.

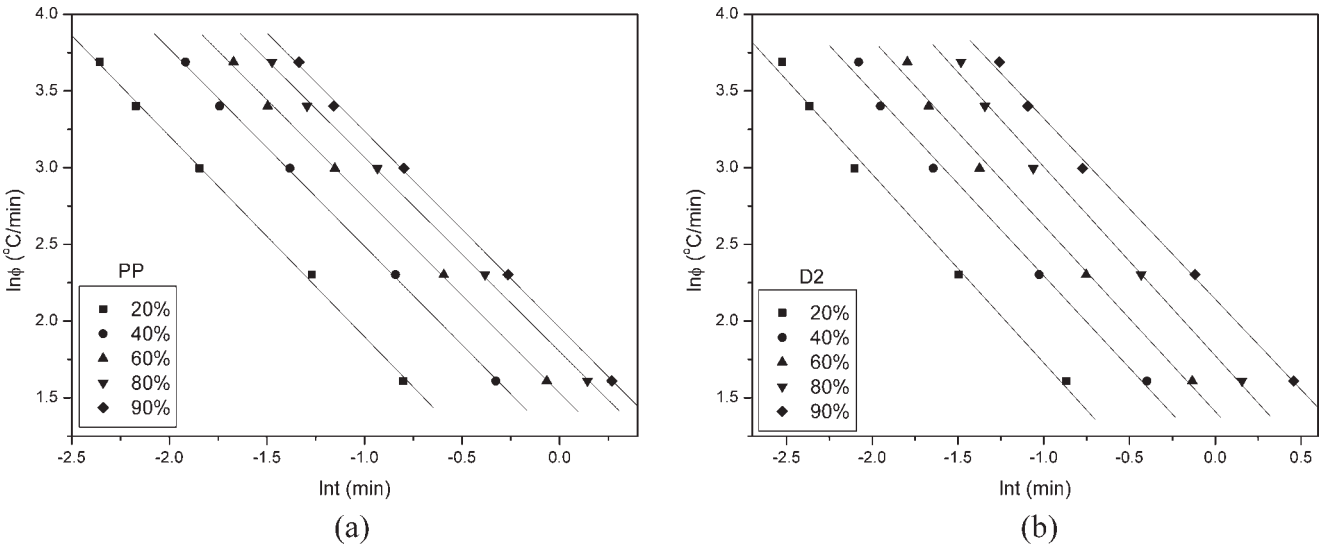

Figure 7 Plots of log ϕ vs. log t for PP and LCB PP: (a) PP; (b) D2.

linearity of these curves suggests that the Ozawa model works very well in describing the nonisothermal crystallization for PP and LCB PPs. Therefore, $K(T)$ and m can be estimated from the intercept and slope, respectively.

To find a method to describe exactly the nonisothermal crystallization process, Mo and coworkers[19] proposed a novel kinetics equation by combing Avrami and Ozawa equation. Under certain crystallinity, Avrami and Ozawa equation have the relationship as shown as follows:

$$\ln Z_t + n \ln t = \ln K(T) - m \ln \phi \tag{8}$$

by rearrangement at a given crystallinity X_t

$$\ln \phi = \ln F(T) - \alpha \ln t \tag{9}$$

where $F(T) = [K(T)/Z_t]^{1/m}$ refers to the value of cooling rate chosen at unit crystallization time when the measured system has a defined degree of crystallinity. $\alpha = n/m$, the ratio of Avrami exponent n to Ozawa exponent m. According to eq. (9), at a given crystallinity, plotting ln ϕ vs. ln t (Fig. 7) gives a linear relationship between ln ϕ and ln t. The kinetic parameter $F(T)$ and α can be determined from the intercept and slope of the lines, respectively, (Table V). It can be seen from Table V that the values of $F(T)$ increase gradually with relative crystallinity increasing, while the values of α are almost constant. At a given degree of crystallinity, the higher the $F(T)$ value, the higher cooling rate is needed within unit crystallization time, indicating the difficulty of polymer crystallization.[20] By comparing the values of $F(T)$ for linear PP and LCB PPs, it was found that the values of $F(T)$ for PP were higher than that for LCB PPs at lower relative crystallinity (≤80%), whereas it became lower than that of LCB PPs with relative crystallinity increasing. This result indicates that the presence of LCB accelerates crystallization of PP at early stage, and then reversed effect on crystallization was exhibited at later stage. The crystallization rate is controlled by nucleation at early stage, while it is controlled by crystalline growth at later stage. For LCB PP, heterogeneous nucleation accelerated the crystallization rate, which exhibited at early stage; however, more nucleation sites, which can be verified by following POM observation, baffled further growth of crystalline, which exhibited at later stage. The trend of $F(T)$ at later stage of crystallization responds to the shoulder in Figure 2(b) or

TABLE V
Parameters from the Mo and Kissinger Analysis

Samples	X_t (%)	$F(T)$	α	ΔE (kJ/mol)
PP	20	1.80	1.31	204.0
	40	3.33	1.29	
	60	4.62	1.27	
	80	6.06	1.27	
	90	7.08	1.28	
D1	20	1.61	1.22	247.3
	40	2.93	1.18	
	60	4.07	1.18	
	80	5.68	1.22	
	90	8.09	1.15	
D2	20	1.64	1.23	240.4
	40	2.98	1.20	
	60	4.10	1.21	
	80	5.89	1.23	
	90	8.52	1.18	
D3	20	1.66	1.21	239.0
	40	2.88	1.20	
	60	4.08	1.21	
	80	6.24	1.19	
	90	8.55	1.17	

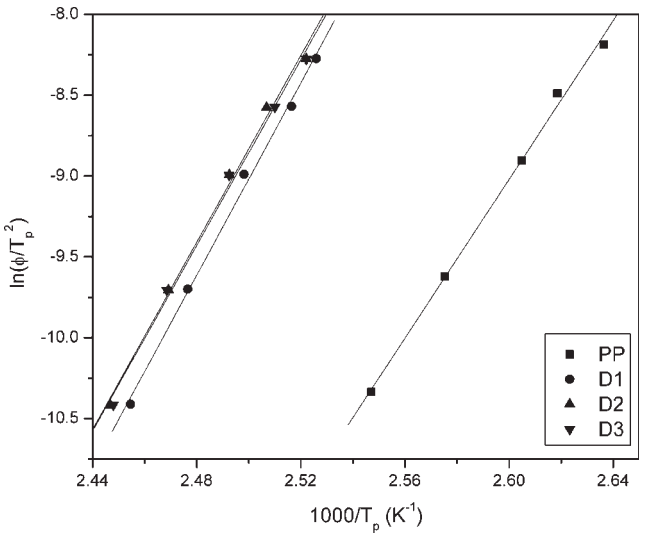

Figure 8 Plots of $\ln(\phi/T_p^2)$ vs. $1/T_p$ for PP and LCB PPs.

slow transition in Figure 3(b) for LCB PP. This result confirms further that the crystallization kinetic process of PP was affected by LCB structure.

Kissinger[21] proposed a method to determine the activation energy (ΔE) for the transport of the macromolecular segments to the growth surface by calculating the variation of the crystallization peak temperature with the cooling rate. The formula can be given as:

$$\frac{d\left[\ln\left(\phi/T_p^2\right)\right]}{d(1/T_p)} = \frac{-\Delta E}{R} \tag{10}$$

where R is the gas constant and T_p is the crystallization peak temperature. The plots of $\ln(\phi/T_p^2)$ vs. $1/T_p$ for PP and LCB PPs were shown in Figure 8 and good linear relations were obtained. The activation energy can be calculated from the slops of these lines and the values of ΔE for PP and LCB PPs were listed in Table V. The values of ΔE for LCB PPs are higher than that for PP, indicating that the presence of LCB baffled the transfer of macromolecular segments from PP melt to the crystal growth surface, which is consistent with the analysis about $F(T)$. The same result was obtained by Zeng et al.[22] In their article, the crystal growth was observed by POM, and they found that the crystal growth rate of linear PP is always faster than that of LCB PP at all crystallization temperatures. Moreover, ΔE of D2 and D3 are lower that of D1, indicating that ΔE decreased slightly with LCB level increasing.

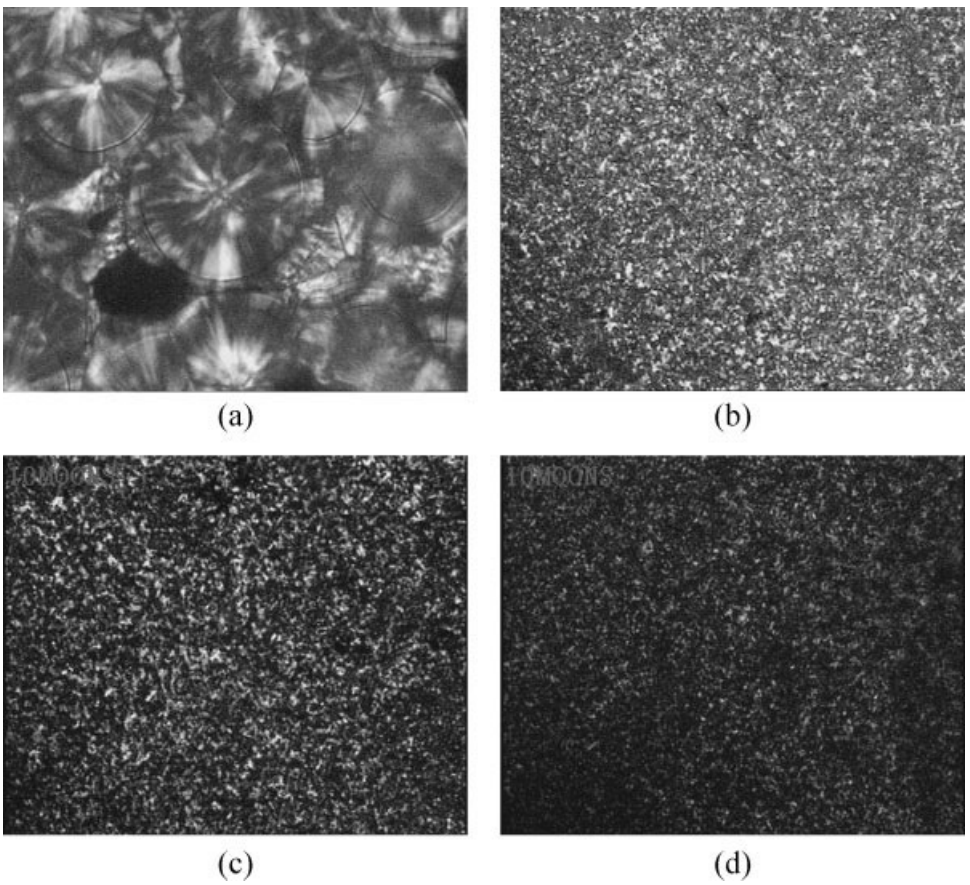

Figure 9 POM micrographs of PP and LCB PPs nonisothermal crystallized at 20°C/min from melt: (a) PP; (b) D1; (c) D2; (d) D3.

From the earlier discussion, it can be found that the nonisothermal crystallization kinetic parameters and ΔE changed slightly with LCB level increasing. It can be explained that the LCB level is very low, the increase of LCB level in so limited degree have a little effect on the crystallization of PP.

Observation of crystal morphology by POM

The crystal morphology of PP and LCB PPs was observed through POM. Figure 9 shows the polarized micrographs of PP and LCB PPs nonisothermal crystallized at a cooling rate of 20°C/min. The linear PP shows well-defined spherulites with a ''Maltese-cross'' structure, whereas LCB PPs show more nucleation sites and very tiny crystallites, indicating that LCB structure acts as a nucleating agent. It can be observed that the introducing of LCB accelerated the nucleation, but the radial growth rate of the spherulites decreased. This observation agrees with the analysis about nonisothermal kinetic parameters. On the other hand, it was observed that the spherulitic development of PP arise from sporadic nucleation, while that of LCB PP arise from instantaneous nucleation. Homogeneous nucleation starts spontaneously by chain aggregation below the melting point, which requires a longer time, whereas heterogeneous nucleation forms simultaneously as soon as the sample reaches the crystallization temperature.[23] Considering the above-mentioned kinetic analysis, it can be concluded that LCB PP crystallizes mainly via heterogeneous nucleation, while PP crystallizes via both heterogeneous nucleation and homogeneous nucleation.

CONCLUSIONS

The nonisothermal crystallization kinetics of linear PP and LCB PPs were investigated systematically by the DSC technique. The results show that at various cooling rates, the exothermic peaks of LCB PPs distinctly shifted to higher temperatures compared with that of linear PP. The Avrami, Jeziorny, Ozawa, and Mo methods can describe the nonisothermal crystallization process of linear PP and LCB PP very well. The Avrami exponent n of LCB PPs is smaller than that of linear PP at various cooling rate, indicating that the introducing of LCB influences the mechanism of nucleation and the growth of PP, moreover, the cooling rate has weak effect on the value of n for LCB PPs compared to linear PP. The value of Z_c for LCB PPs is higher than that for linear PP and the value of $t_{1/2}$ for LCB PPs is lower than that for linear PP, suggesting that the branches have the role of heterogeneous nucleating agent and accelerated the crystallization process. The activation energy ΔE of linear PP and LCB PPs was calculated using Kissinger method. The result shows that the values of ΔE for LCB PPs are higher than that for PP, indicating that the presence of LCB baffled the transfer of macromolecular segments from PP melt to the crystal growth surface. Moreover, the value of ΔE decrease slightly with LCB level increasing. The crystal morphology of PP and LCB PPs was observed through POM. The results show that the spherulites of LCB PPs are much smaller than that of PP, indicating that LCB structure acts as nucleating agent.

References

1. Lagendijk, R. P.; Hogt, A. H.; Buijtenhuijs, A.; Gotsis, A. D. Polymer 2001, 42, 10035.
2. Graebling, D. Macromolecules 2002, 35, 4602.
3. Auhl, D.; Stange, J.; Münstedt, H. Macromolecules 2004, 37, 9465.
4. Gotsis, A. D.; Zeevenhoven, B. L. F.; Tsenoglou, C. J Rheol 2004, 48, 895.
5. Yoshii, F.; Makuuchi, K.; Shingo, K. J Appl Polym Sci 1996, 60, 617.
6. Sugimoto, M.; Tanaka, T.; Masubuchi, Y. J Appl Polym Sci 1999, 73, 1493.
7. Tsenoglou, C. J.; Gotsis, A. D. Macromolecules 2001, 34, 4685.
8. Güldoğan, Y.; Eğri, S.; Rzaev, Z. M. O.; Piskin, E. J Appl Polym Sci 2004, 92, 3675.
9. Seo, Y.; Kim, J.; Kim, K. U.; Kim, Y. C. Polymer 2000, 41, 2639.
10. Kolodka, E.; Wang, W. J. Zhu, S. P. Macromolecules 2002, 35, 10062.
11. Agarwal, P. K.; Somani, R. H.; Weng, W. Q.; Mehta, A. Macromolecules 2003, 36, 5226.
12. Liu, Z. L.; Meng, B.; Tian, W. D. Mod Plast Process Appl 2002, 14, 17.
13. Tian, J. H.; Wu, Y.; Zhou, C. X. Polymer 2006, 47, 7962.
14. Arroyo, M.; Lopez-Manchado, M. A. Polymer 1997, 38, 5587.
15. Liu, X.; Wu, Q. Eur Polym J 2002, 38, 1383.
16. Weng, W. G.; Chen, G. H.; Wu, D. J. Polymer 2003, 44, 8119.
17. Jeziorny, A. Polymer 1978, 19, 1142.
18. Ozawa, T. Polymer 1971, 12, 150.
19. Liu, J.; Mo, Z.; Wang, S.; Zhang, H. Polym Eng Sci 1997, 37, 568.
20. Jiao, C. M.; Wang, Z. Z.; Liang, X. M.; Hu, Y. Polym Test 2005, 24, 71.
21. Kissinger, H. E. J Res Natl Stand 1956, 57, 217.
22. Zeng, W.; Wang, J.; Feng, Z.; Dong, J.; Yan, S. Colloid Polym Sci 2005, 284: 322.
23. Guan, Y.; Wang, S. Z.; Zheng, A. N.; Xiao, H. N. J Appl Polym Sci 2003, 88, 872.